Received 22 February 2024; revised 5 April 2024; accepted 17 April 2024. Date of publication 22 April 2024; date of current version 27 May 2024.

Digital Object Identifier 10.1109/OJAP.2024.3391835

A Machine Learning Approach to Wireless Propagation Modeling in Industrial Environment

MOHAMMAD HOSSEIN ZADEH, MARINA BARBIROLI, AND FRANCO FUSCHINI

Department of Electrical, Electronic, and Information Engineering "G. Marconi," University of Bologna, 40126 Bologna, Italy

CORRESPONDING AUTHOR: M. H. ZADEH (e-mail: mohammad.hossein3@unibo.it)

This work was supported in part by the European Union under the Italian National Recovery and Resilience Plan (PNRR) of NextGenerationEU, a partnership on "Telecommunications of the Future" (PE00000014—Program "RESTART")—Project Industrial Networks, and in part by the EU COST Action INTERACT (Intelligence-Enabling Radio Communications for Seamless Inclusive Interactions) under Grant CA20120.

ABSTRACT Wireless channel properties in industrial environments can differ from residential or office settings due to the considerable impact of heavy machinery that triggers intricate multipath propagation effects and strong blockage effects. Previous investigations on wireless propagation in factories often consisted of empirical models, that is simple analytical formulas based on measurement data. Unfortunately, they usually lack in flexibility, since they seldom include geometrical parameters describing the industrial scenario and therefore turn out reliable only in industrial scenarios sharing the same propagation characteristics as those where the measurements were performed. In response to this limitation, this article harnesses the power of Machine Learning to model propagation markers like path loss, shadowing, and delay spread in the industrial environment. By employing Machine Learning techniques, the objective is to achieve flexibility and adaptability in modeling, enabling the system to effectively generalize across diverse industrial scenarios. The proposed model relies on a combination of predictive algorithms, including a linear regression model and a Multi-Layer Perceptron, working collaboratively to model the relationship between the considered propagation markers and input features like frequency and machine size, spacing, and density. Results are in fair overall agreement with previous studies and highlight some trends about the sensitivity of the propagation parameters to the considered input features.

INDEX TERMS Delay spread, industrial environment, machine learning, path loss, shadowing, wireless propagation channel.

I. INTRODUCTION

WIRELESS communication in industrial manufacturing has advanced in recent years, inspired by the growing popularity of the smart factory idea, where data exchange between machines and controllers (either human or unmanned) is continually carried out not only to improve the whole production process [1], [2] but also to trigger safer work procedures. Wireless solutions can be effectively employed for many applications in industrial environments, like monitoring and surveillance, smart metering, cable replacement, remote control, and autonomous robotics [1], [3].

The performance of wireless systems in the industrial environment depends on equipment design and the properties of the wireless channel. Industrial scenarios have specific properties that make wireless propagation somehow peculiar and different from other wireless channels. In general, industrial environments are larger and/or taller than office or residential buildings and are divided into large departments with high ceilings where the machinery is usually arranged according to some roughly regular layout, with long aisles in between for movement of people and transport of materials [4]. Industrial building structures are often made of reinforced concrete to safely support vehicles and heavy machinery. Industrial equipment is usually made of metal, i.e., highly reflective, with size, density, and spatial distribution that can change significantly case by case. These characteristics of the industrial environment lead to fading Path Loss (PL), obstruction level (shadowing), and Delay Spread (DS) different from other indoor scenarios [5].

Several empirical models for PL, shadowing, and DS were achieved based on measurements in various industrial environments [6], [7], [8], [9], [10], [11], [12], [13], [14], [15]. Empirical models often consist of user-friendly, closed-form expressions mainly aimed at catching the average dependence of major propagation markers (like PL) on some simple link parameters (like distance or frequency). The measurement campaigns required for deriving these models usually mean a lot of cost in time and manpower. Moreover, the nature of empirical models implies that they are only suitable and fairly reliable for environments sharing the same propagation characteristics as those where the measurements were performed, which limits their flexibility and adaptability.

Ray Tracing (RT) is an alternative channel modeling technique [16], [17] that tracks all potential optical rays between a transmitter and a receiver for a given number of permitted wave-matter interactions and starting from a site-specific description of both the environment and the antennas. Then, the computation of the rays' (EM field) contributions is based on geometrical optics (GO), uniform theory of diffraction for diffraction (UTD), and can also include diffuse scattering to some extent [18]. PL data, large- and small-scale fading, time/frequency/angular dispersion, and optical visibility can be investigated through RT in almost every propagation scenario and wireless application [19], [20], [21], as RT is a general-purpose approach. However, RT simulations often lead to large, sometimes prohibitive, computational costs and simulation time [22].

There has been increasing interest in Machine Learning (ML) algorithms in electromagnetic propagation over the last years [23], [24], [25], [26]. The use of ML techniques in wireless channel modeling can be extremely beneficial, as ML-based methods can in principle learn the complex relationship between the channel parameters and the properties of the propagation environment. Moreover, they can be aimed at both average and case-specific evaluations. Another significant advantage of ML models is the inference speed: while the training phase may be computationally expensive (often due to very large datasets), querying the output of a trained model is typically computationally light. In this framework, an ML approach to channel modeling can turn out very flexible, as it can in the end contribute to the achievement of simple, closed-form formulas (like empirical models), or result in a black box describing some complex input-output relationship (like RT models).

This paper presents a hybrid scheme integrating RT simulation tools with ML techniques for predictive channel modeling in the industrial environment. In particular, RT enables the generation of reliable, synthetic, tabular propagation data sets that are then used for the training of different ML models. The ML tools are here conceived for the assessment of PL, shadowing standard deviation (σ), and DS based on the value of few, simple parameters like communication frequency and machine density.

The remainder of this paper is organized as follows: Section II contains recent work on ML-based channel modeling. Section III details the specifications of the industrial environment together with the system setup and industrial wireless channel characterization. In Section IV, the machine learning-based approach to channel modeling is presented. In Section V numerical results are presented and discussed. Finally, Section VI concludes the paper with main takeaways and ideas for future work.

II. RELATED WORK

Industrial wireless propagation has been addressed in some previous works, mostly employing experimental investigations carried out in industrial environments [6], [7], [8], [9], [10], [11], [12], [13], [14], [15]. Measurements are usually exploited to tune the path-loss exponent (PLE) in simple PL formulas [6], [8], [9], [10], [11], [12], [13], [15] and/or to estimate other channel parameters like shadowing level [6], [8], [9], [10], [11], [12], [13], [15] or DS [7], [8], [11], [12], [13], [14], [15]. RT simulations have been also relied on for similar assessments [27], [28], [29], [30]. According to the main outcomes resulting from a literature survey and summed up in Table 1, investigations aimed at industrial propagation modeling have been mostly carried out in Line of Sight (LOS) conditions at frequencies up to a few tens of GHz. Not surprisingly, in LOS conditions PLE is equal to about 2, or even sometimes lower,[1] and (σ) is limited to a few dBs. Both these parameters are likely to be greater in NLOS cases. DS in general ranges from a few to some tens of nsec. The sensitivity of the industrial channel coefficients to parameters like frequency and clutter density does not clearly come out from the survey, as both measurements and RT models are inherently case-specific and the available dataset in Table 1 is likely to be too small to highlight consolidated trends. The limited consistency and/or representativeness of results collected from different case studies is often a common, general drawback of any deterministic, site-specific approach.

Over the last years, channel modeling has been heavily relying on ML techniques. In several cases, ML has been considered for PL prediction, mainly in rural, suburban, and urban outdoor scenarios [31], [32], [33], [34], [35], [36], [37], [38], [39], or in other particular cases [40], [41]. Regarding indoor environments, an ML-based PL regression model was proposed in [42] for an office scenario, whereas an ML approach to the classification of indoor spaces inside a university campus is discussed in [43].

To the best of the authors' knowledge, specific investigations on the industrial wireless channel through ML is basically limited to [44], where ML is fundamentally exploited to cluster the power-angle-delay profiles collected

[1]PLE values lower than two correspond to some guiding effect experienced by the wireless signal. In industrial environments, this may occur between the floor and the ceiling of industrial buildings, and/or along the aisles often present between machinery.

TABLE 1. Related studies. (a, b, c, d) refer to specific working conditions in each reference.

Ref.	Approach	Freq. GHz	PLE	Shadowing[dB]	DS_{mean}[ns]	Antenna	Working Condition
[6]	Experimental	0.9 2.4 5.2	$2.7^{(a)}$, $3.2^{(b)}$, $2.7^{(c)}$ $2.4^{(a)}$, $2.8^{(b)}$, $4.3^{(c)}$ $2.5^{(a)}$, $2.2^{(b)}$, $3.7^{(c)}$	$5.7^{(a)}$, $5.6^{(b)}$, $6.9^{(c)}$ $5^{(a)}$, $5.4^{(b)}$, $8.4^{(c)}$ $5.2^{(a)}$, $4.9^{(b)}$, $5.1^{(c)}$	N.A.	Omnidir.	$^{(a)}$LOS $^{(b)}$NLOS Light clutter $^{(c)}$NLOS Heavy clutter
[7]	Experimental	3.1-10.6 3.1-5.5	N.A.	N.A.	$33^{(a)}$ $42^{(b)}$	Omnidir. monopole	$^{(a)}$LOS $^{(b)}$NLOS
[9]	Experimental	4.1	$1.2^{(a)}$ $1.4^{(b)}$ $1.3^{(c)}$ $1.5^{(d)}$	$0.9^{(a,b)}$ $1.8^{(c)}$ $2.3^{(d)}$	$22^{(a)}$ $7.6^{(b)}$ $83.2^{(c)}$ $106.9^{(d)}$	Directive (D) Omnidir. (O)	$^{(a)}$LOS Sparse clutter DO $^{(b)}$LOS Sparse clutter DD $^{(c)}$LOS Dense clutter DO $^{(d)}$LOS Dense clutter DD
[10]	Experimental	1.3	$1.8^{(a,b)}$ $2.4^{(c)}$ $2.8^{(d)}$	$4.5^{(a)}$ $4.4^{(b)}$ $4.7^{(c)}$ $8.1^{(d)}$	N.A.	Discone	$^{(a)}$LOS Light clutter $^{(b)}$LOS Heavy clutter $^{(c)}$NLOS Light clutter $^{(d)}$NLOS Heavy clutter
[11]	Experimental	3.5 38.5 39.5	$2^{(a)}$ $1.9^{(a)}$ $1.8^{(a)}$	$4^{(a)}$ $4.4^{(a)}$ $4.5^{(a)}$	$16^{(a)}$, $16.6^{(b)}$ $13.7^{(a)}$, $14^{(b)}$ $13.9^{(a)}$, $14.5^{(b)}$	Omnidir.	$^{(a)}$LOS $^{(b)}$NLOS
[12]	Experimental	5.85	$2.2^{(a)}$ $4.7^{(b)}$	$2.4^{(a)}$	$26^{(a)}$ $32.5^{(b)}$	Omnidir.	$^{(a)}$Mostly LOS $^{(b)}$Mostly (heavy) NLOS
[13]	Experimental	108	1.7	0.5	22	Horn	LOS
[14]	Experimental	24	N.A.	N.A.	$28^{(a)}$ $41^{(b)}$	Omnidir.	$^{(a)}$LOS $^{(b)}$NLOS)
[15]	Experimental	6 30	$1.9^{(a)}$, $2.6^{(b)}$ $1.9^{(a)}$, $3.2^{(b)}$	$0.9^{(a)}$, $2.9^{(b)}$ $1.4^{(a)}$, $7.7^{(b)}$	$54^{(a)}$, $43^{(b)}$ $43^{(a)}$, $39^{(b)}$	Directive (scanning) Omnidir.	$^{(a)}$LOS $^{(b)}$NLOS (Light clutter)
[27]	Simulation (RT)	28 60	$2^{(a)}$, $2.1^{(b)}$, $2.2^{(c)}$, $5.3^{(d)}$ $2^{(a)}$, $1.9^{(b)}$, $2.3^{(c)}$, $5.7^{(d)}$	$4.3^{(a,b)}$, $7.3^{(c)}$, $9.5^{(d)}$ $4.5^{(a)}$, $4^{(b)}$, $6.3^{(c)}$, $10^{(d)}$	$13.7^{(a)}$, $38.5^{(b)}$, $29.1^{(c)}$, $49.4^{(d)}$ $13.4^{(a)}$, $38.3^{(b)}$, $29.3^{(c)}$, $49.4^{(d)}$	Isotropic	$^{(a)}$LOS Light factory $^{(b)}$LOS Heavy factory $^{(c)}$NLOS Light factory $^{(d)}$NLOS Heavy factory

from a measurement campaign carried out inside an industrial plant based on some common feature (like power or DS), and to associate then each cluster with a representative power-delay-profile. Therefore, the goal in [44] is not to catch the relationship between propagation markers (like PLE, DS, etc.) and the major features of the industrial scenario, which is instead the main issue tackled in this work. According to an assessment framework already experienced in previous investigations [36], [38], RT simulations at different frequencies and on different realizations of the

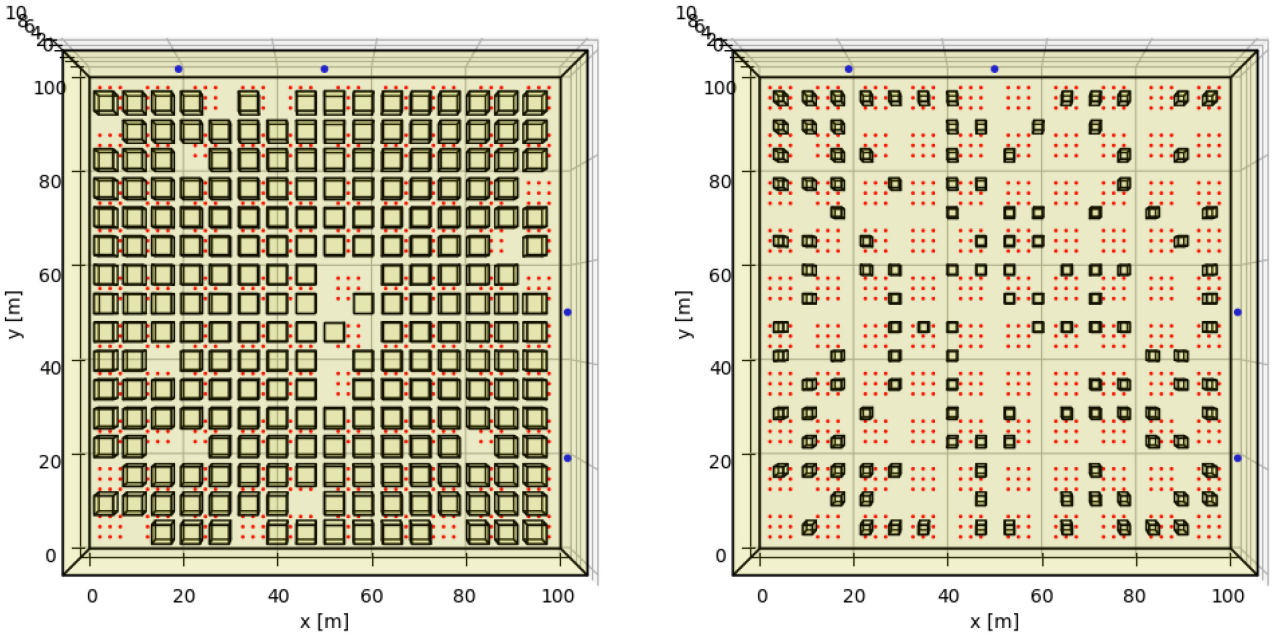

FIGURE 1. Two extreme cases of industrial maps - High Density (MS = 4, SP = 2, T = 0.1, MD = 0.4) and Low Density (MS = 2, SP = 4, T = 0.5, MD = 0.05). Blue and Red points represent the TXs and the RXs, respectively.

industrial environment are leveraged to gather the data required to train and test artificial neural networks (ANN) to learn the dependence of PL, shadowing, and DS on input features like the communication frequency and the machine density. The trained ML networks are then effectively used to complement and further extend the propagation data achieved from RT. Some simple, analytical, parametric formulas for PLE, σ, and DS are finally drawn from such a larger dataset, which includes RT simulation data and ML extrapolated data.

III. ASSESSMENT FRAMEWORK

A. INDUSTRIAL ENVIRONMENT REPRESENTATION

An industrial shed with dimensions of 100 m $\times$ 100 m and a uniform height of 10 m, where machines are all simply represented as metal boxes with te same machine size (MS), machine height (MH), is considered to simulate real-world situations. Machines were at first deployed according to a perfectly regular layout with constant spacing (SP) between them. To make the digital representation of the industrial environment more realistic, a fraction T of machines has been then randomly removed, thus creating some emptier spaces among them.

Multipath propagation in this industrial layout is investigated in this study for different values of MS (2, 3, 4, 8 m), MH (2 m), SP (2, 3, 4m), and T (0.1, 0.2, 0.35, 0.5). An example of two different realizations of the industrial environment is shown in Fig. 1. A total number of 48 scenarios has been then considered, corresponding to the whole set of combinations of these parameters. For each case, five maps have been generated by randomly changing the set of removed machines, for the same T value. The final number of digital maps therefore amounted to 240.

Based on the values of MS, SP, and T, the Machine Density (MD) can be also estimated as:

$$MD \simeq (1 - T) \cdot \left(\frac{MS}{MS + SP} \right)^2 \quad (1)$$

B. TRANSMITTERS, RECEIVERS, AND FREQUENCIES

In this work, transmitters (TXs) are assumed to lie on the shed wall, in four different possible positions (blue points in Fig. 1) at a height of 3 meters above the ground (i.e., slightly higher than MH). For each map, a multitude of receivers (RXs) have been then spread throughout the industrial area at 1 m above ground along the aisles between machines, representing the position of automated guided vehicles (AGVs) often observed in manufacturing and automation scenarios. Four different frequency values have been explored to be used in RT simulations, namely 700 MHz, 3.5 GHz, 28 GHz, and 60 GHz. The selection of these frequencies is driven by the need to assess wireless propagation characteristics for a broad spectrum of possible industrial applications.

C. PROPAGATION MARKERS UNDER INVESTIGATION

Metal is commonly present in industrial scenarios: besides industrial machinery, which is primarily made of metal, metal pipes, shelves, beams, doors, etc. are commonly found in factories. From a propagation perspective, the massive presence of metal parts corresponds to rich multipath effects, i.e., strong reflections and - sometimes - diffractions on metal wedges may trigger the existence of a multitude of different radio paths the wireless signals can follow to effectively propagate through the cluttered industrial environment [1], [4], [5], [6], [7], [11].

Because of multipath interference, the envelope of the received signal exhibits fast and - sometimes deep - spatial fluctuations over distances of the order of the wavelength (small-scale fading), whereas blockage effects result in additional oscillations at a slower rate (large-scale fading) [45]. Because of multipath and blockage effects, the received signal strength decreases with distance only on average. That is, path loss experienced over a link distance d is expressed as:

$$PL(d) = PL(d_0) + 10 \cdot n \cdot \log_{10}\left(\frac{d}{d_0}\right) + \chi \tag{2}$$

where n is the PLE (or propagation factor), $PL(d_0)$ is the PL at a reference distance d_0 and χ is a random variable accounting in general for the spatial fluctuations triggered by large- and small-scale fading. The reference distance is often set as $d_0 = 1m$ and the corresponding loss is then computed through the free space formula, i.e.:

$$PL(d_0) = 20 \cdot \log_{10}\left(\frac{4\pi}{\lambda}\right) \tag{3}$$

In case the values of PL over a multitude of point-to-point links spread over the propagation scenario are collected through measurements or site-specific simulations, the corresponding PLE can be easily computed as:

$$PLE = \frac{\sum_{i=1}^{N}(PL_i - PL(d_0)) \cdot \log_{10}(d_i)}{10\sum_{i=1}^{N}\left(\log_{10}(d_i)\right)^2} \tag{4}$$

being N the number of considered TX-RX links, PL_i and d_i the path-loss value and the TX-RX distance for the i-th considered link.

Finally, it is worth pointing out that the random coefficient χ in eq. (2) is commonly limited to large-scale fading only [4]. To get rid of small-scale fading effects, PL measured or simulated values must be spatially averaged over a small area having a linear dimension equal to several (tens of) λ [45]. Concerning the representation of the industrial scenario considered in this study (Fig. 1), PL point values have been therefore averaged over the 3×3 spatial grids. After the removal of small-scale fading, then $\chi \sim N(0, \sigma)$ [45]. Although attenuation will always represent a crucial issue in wireless communication systems, distortion can also further impair the correct symbol sequence detection at the receiver side. In particular, time dispersion still due to multipath propagation can contribute to the overall degree of distortion to an extent that depends on the DS experienced over the environment and the symbol time length [45]. If M different propagation paths can be identified between a TX and RX pair, and P_i and τ_i represent the intensity and the propagation delay of the i-th path, then:

$$DS = \sqrt{\sum_{i=1}^{M}\frac{P_i}{P} \cdot (\tau_i - \langle\tau\rangle)^2} \tag{5}$$

where $P = \sum_{i=1}^{M} P_i$ and $\langle\tau\rangle = \sum_{i=1}^{M}\frac{P_i}{P} \cdot \tau_i$. Averaging the DS values over many, different TX, and RX pairs leads to a final, mean DS somehow characteristic of the whole propagation environment.

TABLE 2. Simulation configuration.

Parameter Name	Values	
Frequency	0.7, 3.5, 28, 60 GHz	
Antenna Type	Omnidirectional Antenna	
Propagation Mechanism	Direct Ray	On
	Interaction	Up to 4
	Reflection	Up to 3
	Diffraction	Up to 1
	Scattering	Off
	Transmission	Off

IV. MACHINE-LEARNING-BASED PATH LOSS, SHADOWING AND DELAY SPREAD PREDICTION

ML relies on vast datasets and adaptable model architectures to make predictions. In recent times, ML methods have found applications in diverse fields such as self-driving cars, data mining, computer vision, and speech recognition, among others [46]. These applications encompass both supervised and unsupervised learning. In supervised learning, where labeled data is available, the objective is to deduce a generalized and accurate function mapping inputs to outputs. This makes supervised learning well-suited for tackling classification and regression problems. By contrast, unsupervised learning algorithms aim at unraveling the concealed structure within unlabeled data. In essence, PL, shadowing, and DS prediction represent supervised regression problems, which have been here tackled by ANN, and in particular, resorting to Multi-Layer Perceptron (MLP) [47]. Other ML methods, like Support Vector Regression (SVR) [48], XGBR decision trees [49], and Random Forest (RF) [50] have been also considered for the sake of comparison. It has been reported that ML-based models can be more accurate than empirical models and more computationally efficient than deterministic ones [31], [51].

A. RAY TRACING SIMULATION

RT is a powerful computational technique to model the propagation of radio waves in various environments [16], [17]. By simulating the interaction of radio waves with objects and materials in the environment, RT can predict the behavior of wireless communication systems, aiding in their design and optimization. Key parameters in RT simulations include the number of interactions, antenna type, and frequency value. Table 2 summarizes this information for the RT simulations carried out in this work.

RT tools also require the electromagnetic parameters of the materials (relative permittivity ϵ_R and conductivity γ) as input data. In the considered industrial environments, two types of materials are predominantly present. The first type is machinery, which is assumed to be Perfect Electric Conductors (PEC). The second type is the shed, which is assumed made of concrete, with ϵ_R=5, σ=0.01 S/m at lower

TABLE 3. Features.

Features		Values
Environment Dependent	MS	2, 3, 4, 8m
	SP	2, 3, 4m
	MD	[0.05-0.50]
System Dependent	Frequency	0.7, 3.5, 28, 60 GHz

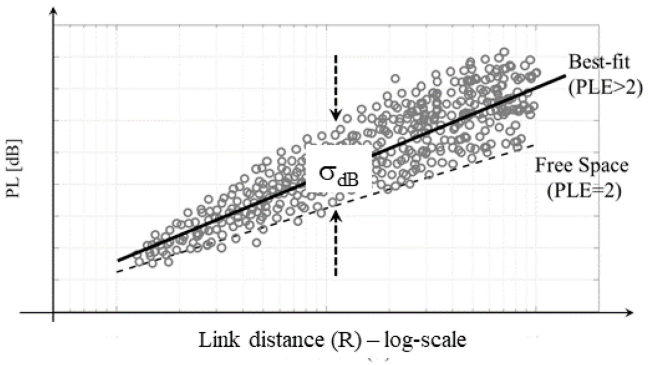

FIGURE 2. Common PL range dependence in wireless channels.

frequencies (0.7 and 3.5 GHz) and σ=0.1 S/m at higher frequencies (28 and 60 GHz).

In this work, several synthetic datasets of the industrial environment have been generated according to the input file format required by the RT tool previously described in [52].

B. DATA COLLECTION AND FEATURE EXTRACTION

The collected data refer to samples obtained from RT simulations, and each sample should include the target output value such as PL, shadowing, and DS and the corresponding input features as mentioned in Table 3.

In the end, the total number RT simulations amounted to 960 (4 frequencies explored over the whole set of 240 digital maps). For each simulation, PL and DS experienced over all the TX-RX links have been computed assuming isotropic antenna at both link ends for the sake of simplicity. The RXs have been grouped in grids of 3 x 3 locations, with distance between the grids equal to 10 m and spacing inside each grid equal to 10λ, being λ the communication wavelength. In this way, fast fading is expected to independently affect the different RXs, and therefore has been filtered out from the simulation results by averaging the PL values over each grid. The corresponding PL values collected over the five simulations sharing the same geometrical parameters have been merged and plotted against link distance in logarithmic scale, for each different frequency (Fig. 2). The final number of collected PLE, σ_{dB}, and DS_{mean} values therefore amounted to 960/5=192 corresponding to the combinations of the features (MS, SP, MD, and frequency). The collected data have been arranged on the dataset sketched in Fig. 3.

The values of PLE, σ_{dB}, and DS_{mean} corresponding to the 192 combinations of the features (MS, SP, MD, and frequency) have been arranged in a database as sketched in Fig. 3.

It is worth pointing out that the size of the database is actually not so large, that in general may not help the accuracy of the ML training stage. The reason is twofold:

- RT simulations for PL modeling are in general not computationally light. Although the RT parameters were set to effectively speed up each single run,[2] the execution of the 960 RT simulations required about two weeks of computation (on a standard PC).
- Each simulation includes four TXs and many RXs (i.e., several hundreds of wireless links) but in the end it contributes to the computation of a single value of PLE, σ_{dB} and DS_{mean}.

C. MODEL SELECTION

The dataset achieved from RT simulations was finally used to train and test an MLP network aimed at catching the relationship between the output label (either PLE, σ_{dB} or DS_{mean}) and the corresponding features. The learning process was organized in three different steps:

1) Since the labels included in the final dataset look somehow linearly dependent on $log_{10}(f_{GHz})$ (Fig. 4), a simple linear regression was first carried out to compute the coefficient β and γ describing the average frequency dependence of the label as::

$$< y >= \beta \cdot log_{10}(f_{GHz}) + \gamma \quad (6)$$

where y indifferently stands for PLE, σ_{dB} or DS_{mean} and $\langle\cdot\rangle$ represents the mean value;

2) for each y_i, i=1,2,.., 192 the residual r_i concerning the regression line has been computed, i.e.:

$$r_i = y_i - \beta \cdot log_{10}(f_{GHz}) - \gamma, \quad \text{i=1, 2,..., 192} \quad (7)$$

3) MLP has been leveraged to seize the dependence of the residuals on the geometrical features (MS, SP, and MD).

Of course, three different MLP networks, respectively tailored to PLE, σ_{dB} or DS_{mean} have been in the end arranged in agreement with the outlined procedure.

D. HYPERPARAMETER SETTING AND MODEL TRAINING

The primary objective during the training stage of every machine learning model is to optimize the parameters, specifically the weights (w) and biases (b) of each layer in MLP, to achieve optimal learning. Following the training stage, the validation phase focuses on fine-tuning hyperparameters such as the number of hidden layers, the neurons within each hidden layer, and the activation function (represented as 'f' in Fig. 5). Table 4 provides a brief summary of the tuned hyperparameters for three distinct models designed for predicting PLE, σ, and DS_{mean}. It is noteworthy that 'ReLU' stands for the Rectifier Linear Unit function, and 'lbfgs' serves as an optimizer from the family of quasi-Newton methods, particularly suitable for small datasets [53], [54].

[2]In particular, the maximum number of bounces permitted for each ray was limited to three, with one diffraction at most. Also, the transmission was not enabled, as the machinery was supposed made of metal.

	MS[m]	SP[m]	MD	freq[GHz]	PLE_{nlos}	PLE_{los}	PLE	$\sigma[dB]_{nlos}$	$\sigma[dB]_{los}$	σ[dB]	DS_{mean}[ns]
0	2	2	0.23	0.7	2.46	1.82	2.30	5.51	3.58	7.01	33.52
1	2	2	0.20	0.7	2.43	1.85	2.29	5.31	3.97	6.68	36.48
2	2	2	0.16	0.7	2.33	1.88	2.23	4.39	3.63	5.40	42.88
3	2	2	0.12	0.7	2.27	1.92	2.19	4.11	3.63	4.75	50.90
4	2	3	0.14	0.7	2.30	1.91	2.18	4.22	3.36	5.03	42.59
...	...	...	...	...	...	...	...	...	...	...	...
187	8	3	0.26	60.0	2.81	2.03	2.68	10.06	3.82	10.64	36.61
188	8	4	0.40	60.0	2.81	2.09	2.72	11.27	3.69	11.32	25.41
189	8	4	0.36	60.0	2.80	2.03	2.67	10.57	3.18	10.89	29.73
190	8	4	0.29	60.0	2.73	2.05	2.60	10.35	4.22	10.55	31.73
191	8	4	0.22	60.0	2.68	2.01	2.47	9.46	4.12	9.87	39.85

FIGURE 3. An example of the dataset considering MS, SP, MD, and frequency as features and PL and Shadowing, and DS as target outputs.

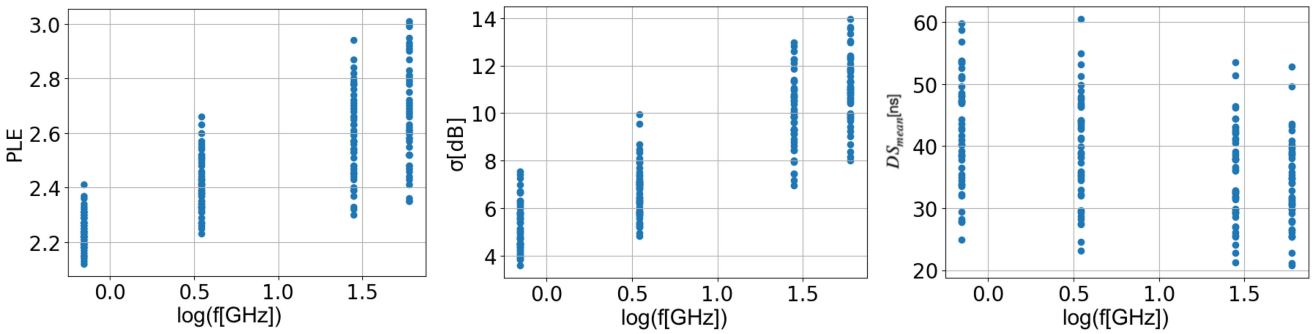

FIGURE 4. Linear relationship between PLE, σ_{dB}, and DS_{mean} Vs. log(f[GHz]).

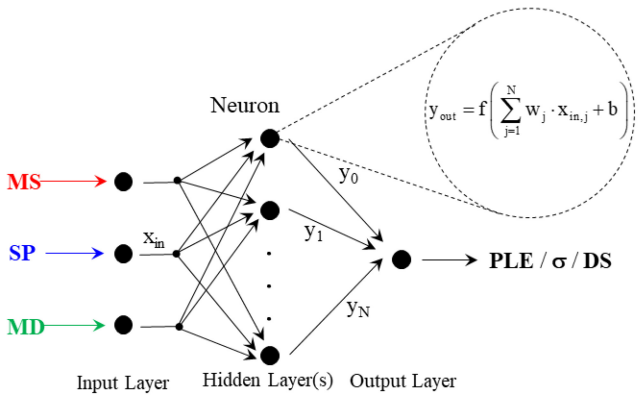

FIGURE 5. General structure of a Multi-Layer Perceptron. A single hidden layer is deployed for the sake of simplicity.

E. MODEL EVALUATION

In general, the performance of regression models is measured by samples in the test dataset, which do not appear in the model training process. The evaluation metrics include prediction accuracy and generalization properties.

In terms of evaluating the accuracy, performance indicators like maximum prediction error, mean absolute error, error standard deviation, correlation factor, root mean square error (RMSE), and mean absolute percentage error are commonly used [31], [51]. In this work RMSE is considered:

$$RMSE(y, \hat{y}) = \sqrt{\frac{1}{n} \cdot \sum (y_i - \hat{y}_i)^2} \tag{8}$$

where y_i is the ground-truth value for input x_i and $\hat{y}_i$ is the predicted value for input x_i and n is the number of samples.

Generalization property describes the model reusability when the deployment concerns new frequency bands and/or new environment types. The model may have better generalization performance with more data collected from diverse scenarios, such as different machine densities and frequencies.

TABLE 4. Major parameters of the neural networks for PLE, σ_{dB} and DS regression.

Hyperparameter	PLE	σ_{dB}	DS
Number of hidden layers	1	1	1
Neurons distribution across the layers	3/3/1	3/4/1	3/4/1
Activation function	tanh	ReLU	tanh
Solver for weight optimization	lbfgs	lbfgs	lbfgs

V. RESULTS AND DISCUSSION

A. NARROWBAND PARAMETERS ASSESSMENT

The accuracy of the ML approach to PLE and σ prediction is displayed in Table 5 in terms of overall loss over the test

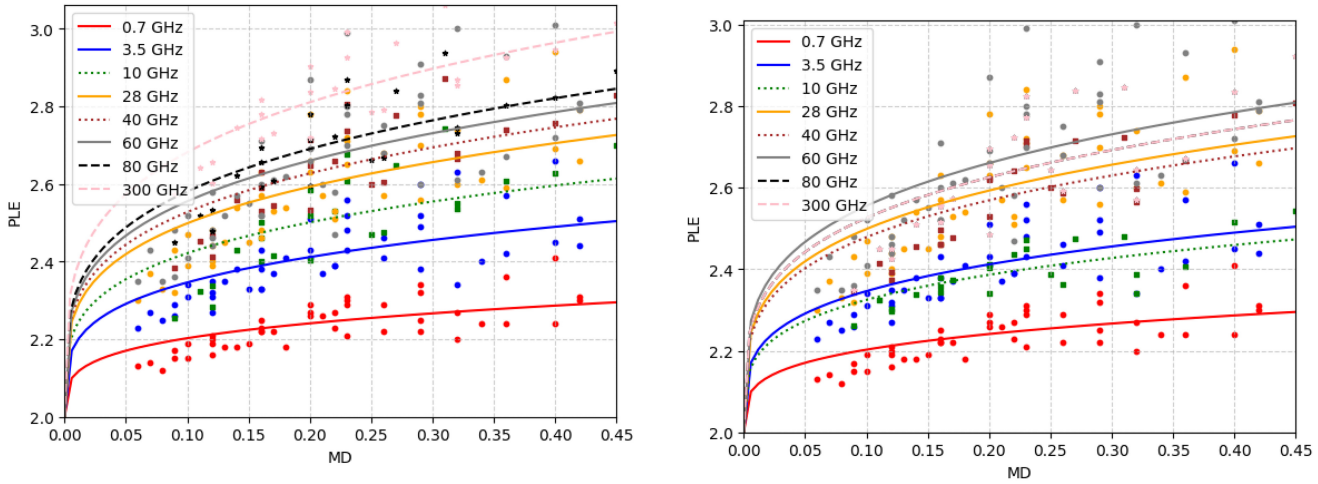

(a) MLP-based model

(b) XGBRegressor

FIGURE 6. PLE sensitivity to MD and frequency for MLP-based model (left) and XGBRegressor (right).

TABLE 5. Model evaluation for PLE and σ and min and max of each case.

	RMSE of different models				Min value	Max value
	MLP	XGBR	SVR	RF		
PLE	0.049	0.051	0.105	0.056	2.12	3.01
σ[dB]	0.630	0.699	1.242	0.751	3.61	13.96

TABLE 6. An example of new dataset.

Features	New values
MS	2.5, 3.5, 6 m
SP	2.5, 3.5 m
frequency	10, 40, 80, 300 GHz

dataset together with the range of variability of each target label. As the loss turns out quite small compared to the range of variability for both parameters, the learning task has been fairly accomplished. Furthermore, a comparison between different models shows satisfactory overall effectiveness, with the MLP and XGBRegressor slightly outperforming the others.

To further investigate and evaluate the models' performances, a generalization perspective is adopted. This entails the evaluation of the models' consistency when challenged on new values of the features never seen during the training stage. To this aim, a fresh dataset with entirely new feature values was considered according to Table 6.

Fig. 6 shows PLE against MD for different frequency values for both the MLP-based model (left) and XGBRegressor (right). Besides the data returned by RT simulations (dots), new data generated utilizing the trained ML tools related to the new dataset (squares and stars) are added to the figures, which also include the corresponding best-fit line. Results are in clear agreement with the RT outcome as far as the MLP-based model is concerned as shown in Fig. 6(a), thus further corroborating the effectiveness of the training but also highlighting a fair robustness in terms of generalization skill. Conversely, the XGBRegressor cannot consistently track the PLE sensitivity to completely new frequency values (Fig. 6(b)). The reason is in the context of the training set, where frequency is represented by four distinct values. Given that XGBRegressor operates on tree-based structures, the decision points for splits in the tree are defined by conditions such as frequency lower and/or greater than a threshold. With only four unique values for frequency, the resulting thresholds in the tree are likely to closely align with these specific values. For instance, consider a split condition frequency greater than 28 GHz and less than 60 GHz, where observations with frequencies 28 GHz and 40 GHz may be grouped on the same branch. In situations where the remaining features exhibit similar characteristics, these two observations are anticipated to receive nearly identical predictions. In conclusion, the MLP-based model turns out as the most reliable and flexible overall and will be therefore referred to in the following.

Fig. 7 shows σ against MD for different frequency values. Similar to the PLE model, they are in clear agreement with the RT outcome as far as the MLP-based model is concerned.

Prior research suggests that conventional ML models excel in interpolating within the known data range but often exhibit poor performance when extrapolating beyond this range [55]. However, the MLP-based model employed in this study is not in agreement with this trend, as it effectively learned the correlation between the target output and frequency, demonstrating a remarkable ability to predict accurately even for frequency values outside the frequency range explored inside the training dataset.

In the end, the trained MLP can be exploited to quickly and reliably complement the limited amount of information that has been painstakingly gathered through electromagnetic simulations (or could be provided by channel experimental sounding). Of course, the availability of a large set of information can help to clearly get a deeper insight into the

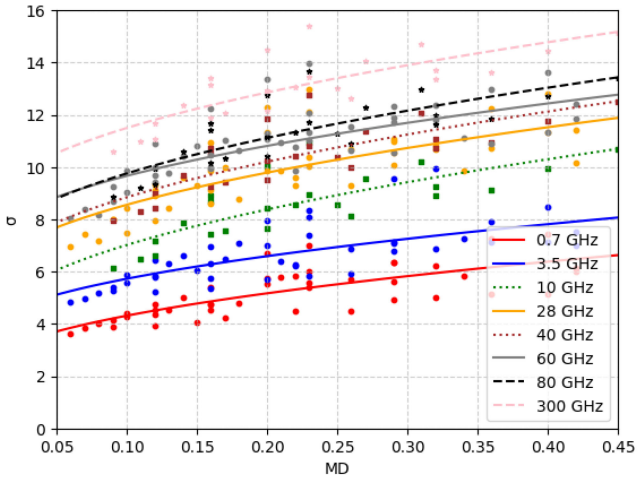

FIGURE 7. σ sensitivity to MD and frequency for MLP-based model.

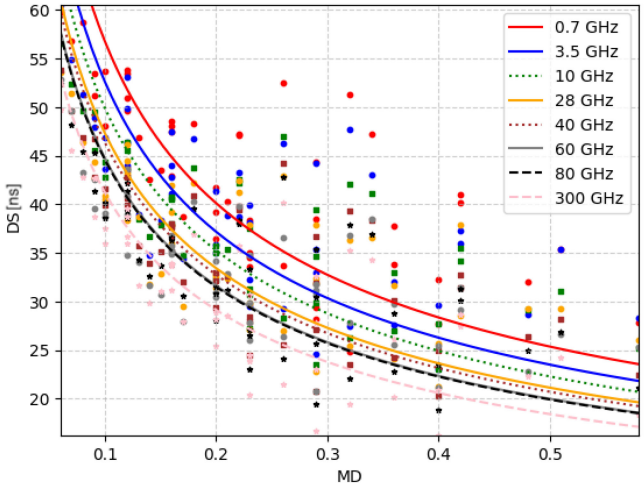

FIGURE 8. DS sensitivity to MD and frequency for MLP-based model.

TABLE 7. Model evaluation for DS_{mean} and min and max values.

	RMSE of different models				Min value	Max value
	MLP	XGBR	SVR	RF		
PLE	0.049	0.051	0.105	0.056	2.12	3.01
σ[dB]	0.630	0.699	1.242	0.751	3.61	13.96

existing relationship between the output propagation labels and the considered input features. For instance, Figs. 6(a) and 7 quite clearly show that both PLE and σ increase with machine density and frequency. Simple best-fit lines have been then computed to formally describe the highlighted trends, e.g., employing the following expressions:

$$PLE = 2 + k_1 \cdot \sqrt[4]{MD \cdot f_{GHz}^{\frac{1}{k_2}}} \tag{9}$$

$$\sigma = k_3 \cdot \sqrt{MD} + k_4 \cdot log_{10}(f_{GHz}) \tag{10}$$

The coefficients $k_1 - k_4$ can be easily computed for each frequency according to the least square method over the corresponding dataset, leading to the continuous and dashed lines in Figs. 6(a) and 7. To get a single, somehow rougher but very simple analytical model, the same coefficients have been also optimized across the whole set of frequencies, corresponding to the final values of $k_1 = 0.48$, $k_2 = 1.5$, $k_3 = 10.27$, and $k_4 = 3.45$.

B. WIDEBAND PARAMETERS ASSESSMENT

Table 7 shows that the learning process can be accomplished also for DS prediction. Although the four considered ML methods turn out quite accurate, the MLP-based model outperforms the others. The model flexibility and consistency are again investigated in Fig. 8, where the DS_{mean} values returned by RT simulations are reported for different MD and frequency together with the values achieved from the trained MLP-based model corresponding to the same new set of features previously referred to (Table 6).

As shown in Fig. 8, the outcomes from the MLP for the values of the fresh features are physically sound and consistent with the RT results. Best-fit lines are also traced in Fig. 8, aimed at highlighting the average dependence of DS_{mean} on MD and frequency. The corresponding analytical formulation is reported in the following eq. (11):

$$DS_{mean} = k_5 \cdot \frac{1}{\sqrt{MD \cdot f_{GHz}^{\frac{1}{k_6}}}} \tag{11}$$

The least square method can be leveraged to compute the best k_5 and k_6 values at each different frequency (continuous and dashed lines in Fig. 8. A simple, average DS prediction formula describing its sensitivity to MD and frequency can be instead achieved by extending the least square computation all over the whole dataset. In this case, the values of the coefficients were found to equal k_5=8.35 and k_6=20.35.

C. COMPARISON WITH PREVIOUS STUDIES

This sub-section discusses the reliability of the proposed ML-based approach to wireless propagation modeling in factories in comparison with the results reported in previous studies (Table 1) and technical report [56].

Experimental and simulation assessments summarized in Table 1 show that in the presence of LoS, PLE is approximately equal to 2 regardless of the frequency (green crosses in Fig. 9), whereas in NLoS conditions it is increasingly greater as the NLoS level gets heavier (red dots and purple stars in Fig. 9). Also, PLE significantly increases with frequency in the case of dense industrial clutter (purple stars in Fig. 9). These trends are actually in contrast with the path-loss models for indoor factories included in [56], where a PLE independent of frequency is instead assumed, and the value corresponding to sparse clutter is greater than that considered for dense clutter. Also, PLE values in [56] for the industrial case are just slightly greater than 2 even in NLoS conditions, which sounds somehow unlikely.

In this framework, the results returned by the proposed MLP-based model look like a sort of trade-off between

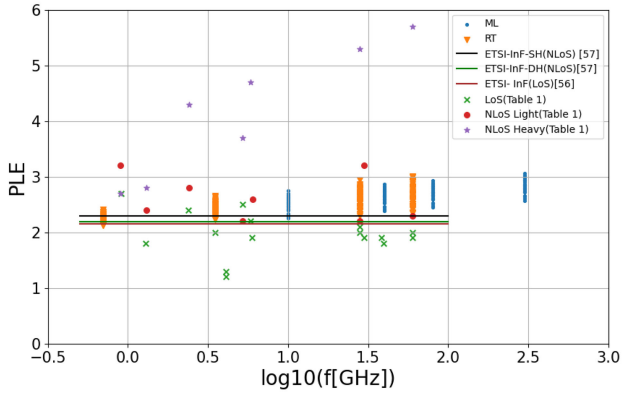

FIGURE 9. Model - literature comparison for path loss exponent.

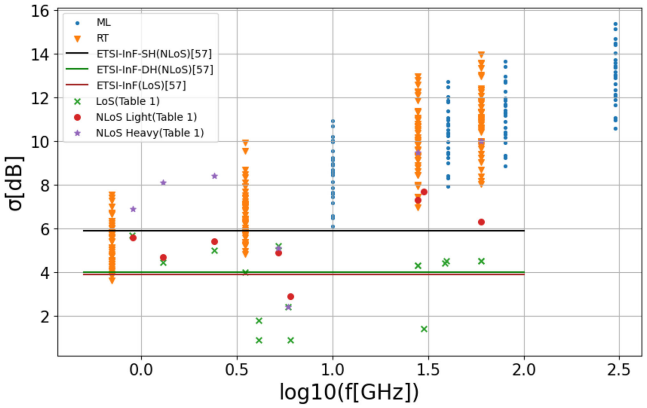

FIGURE 10. Model - literature comparison for shadowing level.

previous evaluations, showing a PLE that slightly increases with frequency (Fig. 9) and machine density (Fig. 6(a)). Moreover, since the PLE values referring to RT and ML model in Fig. 9 correspond to LoS and NLoS altogether, it is not surprising they are on the average in between PLE values achieved for LoS and (heavy) NLoS conditions separately.

Rather similar considerations hold for the assessment of shadowing level, as reported in Fig. 10. It is worth reminding that the values of σ_{dB} corresponding to RT and ML in Fig. 10 again refer to LoS and NLoS altogether, which may explain why values greater than those limited to LoS or NLoS only have been sometimes achieved.

Finally, a comparison in terms of DS is shown in Fig. 11. Since the values of DS in Table 1 for NLoS conditions are seldom related to the corresponding clutter level, Fig. 11 simply considers LoS and NLoS classes. Results returned by RT and ML assessment are in fair agreement with previous experimental analyses (green crosses and red dots in the figure), suggesting a slight reduction of DS for increasing frequency. This was already clear in Fig. 7, where the difference between mean DS at 0.7 GHz and 300 GHz amounts to about 7 nsec only. Comparison with the simple formulas for mean DS included in [56] looks a bit worse, but anyway acceptable. In fact, the DS standard deviation

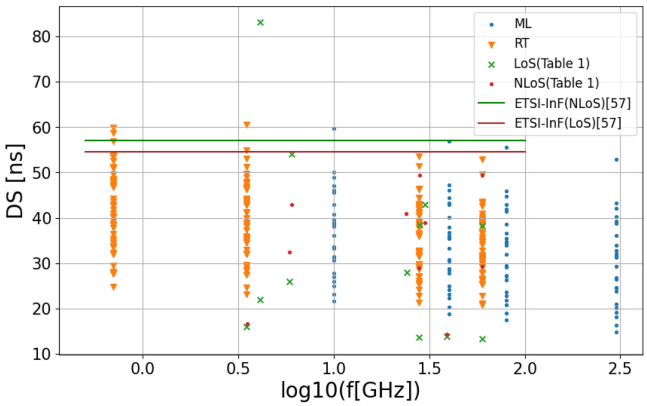

FIGURE 11. Model - literature comparison for DS.

reported in [56] (σ_{DS}) is equal to about 18 nsec. (for both LoS and NLoS cases), thus meaning that most of the values returned by the joint RT and ML approach actually belong to the $\pm\sigma_{DS}$ range around the average values suggested in [56].

It is finally worth noting that although the learning process was based on data collected from simulations carried out for the same size of the industrial shed, results discussed in this section have turned out to be in general agreement with previous model and experimental investigations clearly referred to different industrial environments and machinery layout. This confirms the model is flexible and versatile, and suggests it has fair generalization skills also in the environment domain.

VI. CONCLUSION

In this work, narrowband and wideband propagation modeling in an industrial environment has been addressed by employing an ML-based approach including a simple linear regression and a multi-layer perceptron network. Training data have been achieved through ray-tracing simulations carried out at different frequencies and on several realizations of the industrial context. Satisfactory performance of the ML model has been achieved, both in terms of interpolation and extrapolation skills. Overall, the results are quite in agreement with previous investigations and existing models. Moreover, the trained neural network has been queried to complement the outcomes of RT simulations, therefore achieving a large(r) database accounting for the complex relationship between propagation markers like path loss exponent, shadowing level, and DS and features like frequency and machine size, spacing and density. Based on this extended dataset, simple, closed-form formulas to estimate the values of path loss exponent, shadowing level, and DS from machine density and communication frequency have been also proposed. Both path-loss exponent and shadowing std. deviations increase at a larger frequency and machine density, whereas an opposite trend has been found for DS. Although the sensitivity of the considered propagation parameters to the height of antennas and machinery has not been considered to limit the computational effort, it

clearly represents an interesting issue that deserves further investigation as well as the impact of antenna radiation patterns on the properties of the industrial wireless channel.

REFERENCES

[1] S. Vitturi, F. Tramarin, and L. Seno, "Industrial wireless networks: The significance of timeliness in communication systems," *IEEE Ind. Electron. Mag.*, vol. 7, no. 2, pp. 40–51, Jun. 2013.

[2] V. K. L. Huang, Z. Pang, C.-J. A. Chen, and K. F. Tsang, "New trends in the practical deployment of industrial wireless," *IEEE Ind. Electron. Mag.*, vol. 12, no. 2, pp. 50–58, Jun. 2018.

[3] M. Cheffena, "Industrial wireless communications over the millimeter wave spectrum: Opportunities and challenges," *IEEE Commun. Mag.*, vol. 54, no. 9, pp. 66–72, Sep. 2016.

[4] M. Cheffena, "Propagation channel characteristics of industrial wireless sensor networks," *IEEE Antennas Propag. Mag.*, vol. 58, no. 1, pp. 66–73, Feb. 2016.

[5] P. Stenumgaard, J. Chilo, J. Ferrer-Coll, and P. Angskog, "Challenges and conditions for wireless machine-to-machine communications in industrial environments," *IEEE Commun. Mag.*, vol. 51, no. 6, pp. 187–192, Jun. 2013.

[6] E. Tanghe et al., "The industrial indoor channel: Large-scale and temporal fading at 900, 2400, and 5200 MHz," *IEEE Trans. Wireless Commun.*, vol. 7, no. 7, pp. 2740–2751, Jul. 2008.

[7] J. Karedal, S. Wyne, P. Almers, F. Tufvesson, and A. F. Molisch, "A measurement-based statistical model for industrial ultra-wideband channels," *IEEE Trans. Wireless Commun.*, vol. 6, no. 8, pp. 3028–3037, Aug. 2007.

[8] Y. Ai, J. B. Andersen, and M. Cheffena, "Path-loss prediction for an industrial indoor environment based on room electromagnetics," *IEEE Trans. Antennas Propag.*, vol. 65, no. 7, pp. 3664–3674, Jul. 2017.

[9] B. B. Cebecioglu et al., "Sub-6 GHz channel modeling and evaluation in indoor industrial environments," *IEEE Access*, vol. 10, pp. 127742–127753, 2022.

[10] T. S. Rappaport and C. D. McGillem, "UHF fading in factories," *IEEE J. Sel. Areas Commun.*, vol. 7, no. 1, pp. 40–48, Jan. 1989.

[11] Y. Wang, Y. Lv, X. Yin, and J. Duan, "Measurement-based experimental statistical modeling of propagation channel in Industrial IoT scenario," *Radio Sci.*, vol. 55, no. 9, pp. 1–14, Sep. 2020.

[12] B. Holfeld et al., "Radio channel characterization at 5.85 GHz for wireless M2M communication of industrial robots," in *Proc. IEEE Wireless Commun. Netw. Conf.*, 2016, pp. 1–7, doi: 10.1109/WCNC.2016.7564890.

[13] A. Al-Saman, M. Mohamed, M. Cheffena, and A. Moldsvor, "Wideband channel characterization for 6G networks in industrial environments," *Sensors* vol. 21, no. 6, Mar. 2021.

[14] S. R. Panigrahi, N. Bjorsell, and M. Bengtsson, "Power delay profile investigation in industrial indoor environments at the 24 GHz ISM band," in *Proc. IEEE Int. Conf. Ind. Technol. (ICIT)*, 2022, pp. 1–6, doi: 10.1109/ICIT48603.2022.10002732.

[15] D. Dupleich, R. Müller, M. Landmann, J. Luo, G. D. Galdo, and R. S. Thomä, "Multi-band characterization of propagation in industry scenarios," in *Proc. 14th Eur. Conf. Antennas Propagat., Copenaghen*, 2020, pp. 1–5, doi: 10.23919/EuCAP48036.2020.9135630.

[16] Z. Yun and M. F. Iskander, "Ray tracing for radio propagation modeling: Principles and applications," *IEEE Access*, vol. 3, pp. 1089–1100, 2015, doi: 10.1109/ACCESS.2015.2453991.

[17] J. W. McKown and R. L. Hamilton, "Ray tracing as a design tool for radio networks," *IEEE Netw.*, vol. 5, no. 6, pp. 27–30, Nov. 1991.

[18] E. M. Vitucci, N. Cenni, F. Fuschini, and V. Degli-Esposti, "A reciprocal heuristic model for diffuse scattering from walls and surfaces," *IEEE Trans. Antennas Propag.*, vol. 71, no. 7, pp. 6072–6083, Jul. 2023, doi: 10.1109/TAP.2023.3278796.

[19] M. F. Catedra, J. Perez, F. Saez de Adana, and O. Gutierrez, "Efficient ray-tracing techniques for three-dimensional analyses of propagation in mobile communications: Application to picocell and microcell scenarios," *IEEE Antennas Propag. Mag.*, vol. 40, no. 2, pp. 15–28, Apr. 1998.

[20] Y. Hwang, Y. P. Zhang, and R. G. Kouyoumjian, "Ray-optical prediction of radio-wave propagation characteristics in tunnel environments. 1. Theory," *IEEE Trans. Antennas Propagat.*, vol. 46, no. 9, pp. 1328–1336, Sep. 1998.

[21] F. Fuschini, M. Barbiroli, G. Bellanca, G. Calò, J. Nanni, and V. Petruzzelli, "A ray tracing tool for propagation modeling in layered media: A case study at the chip scale," *IEEE Open J. Antennas Propag.*, vol. 3, pp. 249–262, 2022, doi: 10.1109/OJAP.2022.3148855.

[22] V. Degli-Esposti, F. Fuschini, E. M. Vitucci, and G. Falciasecca, "Speed-up techniques for ray tracing field prediction models," *IEEE Trans. Antennas Propagat.*, vol. 57, no. 5, pp. 1469–1480, May 2009, doi: 10.1109/TAP.2009.2016696.

[23] A. Seretis and C. D. Sarris, "An overview of machine learning techniques for radio wave propagation modeling," *IEEE Trans. Antennas Propag.*, vol. 70, no. 6, pp. 3970–3985, Jun. 2022.

[24] D. C. Nguyen et al., "Enabling AI in future wireless networks: A data life cycle perspective," *IEEE Commun. Surveys Tuts.*, vol. 23, no. 1, pp. 553–595, 1st Quart., 2021, doi: 10.1109/COMST.2020.3024783.

[25] C. Huang et al., "Artificial intelligence enabled radio propagation for communications—Part I: Channel characterization and antenna-channel optimization," *IEEE Trans. Antennas Propag.*. vol. 70, no. 6, pp. 3939–3954, Jun. 2022, doi: 10.1109/TAP.2022.3149663.

[26] C. Huang et al., "Artificial intelligence enabled radio propagation for communications—Part II: Scenario identification and channel modeling," *IEEE Trans. Antennas Propag.*, vol. 70, no. 6, pp. 3955–3969, Jun. 2022, doi: 10.1109/TAP.2022.3149665.

[27] D. Solomitckii, A. Orsino, S. Andreev, Y. Koucheryavy, and M. Valkama, "Characterization of mmWave channel properties at 28 and 60 GHz in factory automation deployments," in *Proc. IEEE Wireless Commun. Netw. Conf. (WCNC)*, 2018, pp. 1–6, doi: 10.1109/WCNC.2018.8377337.

[28] J. Yang et al., "Ultra-reliable communications for industrial Internet of Things: Design considerations and channel modeling," *IEEE Netw.*, vol. 33, no. 4, pp. 104–111, Jul./Aug. 2019, doi: 10.1109/MNET.2019.1800455.

[29] G. S. Bhatia, Y. Corre, and M. Di Renzo, "Efficient ray-tracing channel emulation in industrial environments: An analysis of propagation models impact," in *Proc. Joint Eur. Conf. Netw. Commun. 6G Summit (EuCNC/6G Summit)*, 2023, pp. 180–185, doi: 10.1109/EuCNC/6GSummit58263.2023.10188258.

[30] M. U. Sheikh, K. Ruttik, R. Jäntti, and J. Hämäläinen, "Blockage and ray tracing propagation model in 3GPP specified industrial environment," in *Proc. Int. Conf. Inf. Netw. (ICOIN)*, 2021, pp. 397–402, doi: 10.1109/ICOIN50884.2021.9333909.

[31] E. Ostlin, H.-J. Zepernick, and H. Suzuki, "Macrocell path-loss prediction using artificial neural networks," *IEEE Trans. Veh. Technol.*, vol. 59, no. 6, pp. 2735–2747, Jul. 2010, doi: 10.1109/TVT.2010.2050502.

[32] C. A. Oroza, Z. Zhang, T. Watteyne, and S. D. Glaser, "A machine-learning based connectivity model for complex terrain large-scale low-power wireless deployments," *IEEE Trans. Cogn. Commun. Netw.*, vol. 3, no. 4, pp. 576–584, Dec. 2017, doi: 10.1109/TCCN.2017.2741468.

[33] I. Popescu, D. Nikitopoulos, P. Constantinou, and I. Nafornita, "ANN prediction models for outdoor environment," in *Proc. IEEE 17th Int. Symp. Pers., Indoor, Mobile Radio Commun.*, 2006, pp. 1–5, doi: 10.1109/PIMRC.2006.254270.

[34] M. Ayadi, A. Ben Zineb, and S. Tabbane, "A UHF path loss model using learning machine for heterogeneous networks," *IEEE Trans. Antennas Propag.*, vol. 65, no. 7, pp. 3675–3683, Jul. 2017, doi: 10.1109/TAP.2017.2705112.

[35] M. González-Palacio, D. Tobón-Vallejo, L. M. Sepúlveda-Cano, S. Rúa, and L. B. Le, "Machine-learning-based combined path loss and shadowing model in LoRaWAN for energy efficiency enhancement," *IEEE Internet Things J.*, vol. 10, no. 12, pp. 10725–10739, Jun. 2023, doi: 10.1109/JIOT.2023.3239827.

[36] I. F. M. Rafie, S. Y. Lim, and M. J. H. Chung, "Path loss prediction in urban areas: A machine learning approach," *IEEE Antennas Wireless Propag. Lett.*, vol. 22, no. 4, pp. 809–813, Apr. 2023, doi: 10.1109/LAWP.2022.3225792.

[37] A. Gupta, J. Du, D. Chizhik, R. A. Valenzuela, and M. Sellathurai, "Machine learning-based urban canyon path loss prediction using 28 GHz manhattan measurements," *IEEE Trans. Antennas Propag.*, vol. 70, no. 6, pp. 4096–4111, Jun. 2022, doi: 10.1109/TAP.2022.3152776.

[38] K. Mao et al., "Machine-learning-based 3D channel modeling for U2V mmWave communications," *IEEE Internet Things J.*, vol. 9, no. 8, pp. 17590–17607, Sep. 2022, doi: 10.1109/JIOT.2022.3155773.

[39] Y. Zhang, J. Wen, G. Yang, and Z. He, "Air-to-air path loss prediction based on machine learning methods in urban environments," *Wireless Commun. Mobile Comput.*, vol. 2018, Jun. 2018, Art. no. 8489326.
[40] A. Seretis, V. Jevremovic, A. Jemmali, and C. D. Sarris, "Generalizable machine-learning-based modeling of radio wave propagation in stadiums," *IEEE Open J. Antennas Propag.*, vol. 4, pp. 1116–1128, 2023, doi: 10.1109/OJAP.2023.3310382.
[41] D. Wu, G. Zhu, and B. Ai, "Application of artificial neural networks for path loss prediction in railway environments," in *Proc. 5th Int. ICST Conf. Commun. Netw.*, 2010, pp. 1–5.
[42] T. Popescu, D. Nikitopoulos, I. Nafornita, and P. Constantinou, "ANN prediction models for indoor environment," in *Proc. IEEE Int. Conf. Wireless Mobile Comput., Netw. Commun.*, 2006, pp. 366–371.
[43] M. I. AlHajri, N. T. Ali, and R. M. Shubair, "Classification of indoor environments for IoT applications: A machine learning approach," *IEEE Antennas Wireless Propag. Lett.*, vol. 17, pp. 2164–2168, 2018, doi: 10.1109/LAWP.2018.2869548.
[44] M. Kashef, P. Vouras, R. D. Jones, R. Candell, and K. A. Remley, "A machine-learning approach for the exemplar extraction of mmWave industrial wireless channels," *IEEE Open J. Instrum. Meas.*, vol. 1, pp. 1–15, Jun. 2022, doi: 10.1109/OJIM.2022.3181309.
[45] H. L. Bertoni, "Survey of observed characteristics of the propagation channel," in *Radio Propagation for Modern Wireless Systems*. Hoboken, NJ, USA: Prentice Hall, 2000.
[46] Y. Zhang, J. Wen, G. Yang, Z. He, and J. Wang, "Path loss prediction based on machine learning: Principle, method, and data expansion," *Appl. Sci.*, vol. 9, p. 1908, May 2019, doi: 10.3390/app9091908.
[47] M. Popescu, V. Balas, L. Perescu-Popescu, and N. Mastorakis, "Multilayer perceptron and neural networks," *WSEAS Trans. Circuits Syst.*, vol. 8, no. 7, pp. 579–588, 2009.
[48] A.J. Smola and B. Schölkopf, "A tutorial on support vector regression," *Stat. Comput.* vol. 14, pp. 199–222, Aug. 2004, doi: 10.1023/B:STCO.0000035301.49549.88.
[49] T. Chen and C. Guestrin, "XGBoost: A scalable tree boosting system," in *Proc. 22nd ACM SIGKDD Int. Conf. Knowl. Discov. Data Min.*, 2016, pp. 785–794, doi: 10.1145/2939672.2939785.
[50] A. Liaw and M. Wiener, "Classification and regression by randomForest," *R News*, vol. 2, no. 3, pp. 18–22, 2002.
[51] J. Isabona and V. M. Srivastava, "Hybrid neural network approach for predicting signal propagation loss in urban microcells," in *Proc. IEEE Region 10 Humanit. Technol. Conf. (R10-HTC)*, 2016, pp. 1–5.
[52] E. M. Vitucci et al., "Ray tracing RF field prediction: An unforgiving validation," *Int. J. Antennas Propag.*, vol. 2015, pp. 1–11, Aug. 2015.
[53] A. F. Agarap, "Deep learning using rectified linear units (ReLU)," 2019, *arXiv:1803.08375*.
[54] A. S. Berahas, M. Jahani, P. Richtárik, and M. Takáč, "Quasi-newton methods for machine learning: Forget the past, just sample," *Optim. Methods Softw.*, vol. 37, no. 5, pp. 1668–1704, 2022, doi: 10.1080/10556788.2021.1977806.
[55] G. J. Hahn, "The hazards of extrapolation in regression analysis," *J. Qual. Technol.*, vol. 9, no.4, pp. 159–165, 2018, doi: 10.1080/00224065.1977.11980791.
[56] "Study on channel model for frequencies from 0.5 to 100 GHz; (Release 16), Version 16.1.0," ETSI Sophia Antipolis, France, Rep. TR 38.901, 2020.

MOHAMMAD HOSSEIN ZADEH received the M.Sc. degree in telecommunications engineering from the University of Bologna, where he is currently pursuing the Ph.D. degree in telecommunications engineering. His activity is focused on the research topic of Assessment and Development of Channel Modeling by Machine Learning. His research activity includes participation in European research and cooperation programs (COST INTERACT).

MARINA BARBIROLI received the Laurea degree in electronic engineering and the Ph.D. degree in computer science and electronic engineering from the University of Bologna in 1995 and 2000, respectively, where she is currently an Associate Professor with the Department of Electrical, Electronic and Information Engineering "G. Marconi." Her research interests are on propagation models for mobile communications systems, with a focus on wideband channel modeling for 5G systems and beyond. Her research activities include investigation of planning strategies for mobile systems, broadcast systems, and broadband wireless access systems, analysis of exposure levels generated by all wireless systems and for increasing spectrum efficiency. Her research activity includes participation in European research and cooperation programs (COST 259, COST 273 COST2100, COST IC1004, COST IRACON, and COST INTERACT) and the European Networks of Excellence FP6-NEWCOM and FP7-NEWCOM++.

FRANCO FUSCHINI received the M.Sc. degree in telecommunication engineering and the Ph.D. degree in electronics and computer science from the University of Bologna, Italy, in March 1999 and July 2003, respectively, where he is currently an Associate Professor with the Department of Electrical, Electronic and Information Engineering "Guglielmo Marconi." He is the author or a coauthor of about 50 journal articles on electromagnetic wave propagation and wireless systems design. His main research interests are in the areas of radio systems technologies and radio propagation theoretical modeling and experimental investigation. He received the "Marconi Foundation Young Scientist Prize" in the context of the XXV Marconi International Fellowship Award in April 1999.

Open Access funding provided by 'Alma Mater Studiorum - Università di Bologna' within the CRUI CARE Agreement